J|A|C|S COMMUNICATIONS

Published on Web 03/02/2010

The Unusual Electronic Structure of Dinitrosyl Iron Complexes

Shengfa Ye* and Frank Neese*

Lehrstuhl für Theoretische Chemie, Universität Bonn, Bonn D-53115, Germany

Received November 2, 2009; E-mail: shengfa.ye@thch.uni-bonn.de; neese@thch.uni-bonn.de

Nitric oxide (NO) plays a pivotal role in a range of physiological processes such as blood pressure regulation, immune system response, neurotransmission, and smooth muscle relaxation.[1] In NO-mediated degradation of iron−sulfur clusters, the formation of protein bound dinitrosyl iron complexes (DNICs) has been observed.[2] Likewise, modified or damaged iron−sulfur clusters can be reassembled directly from DNICs.[3] In parallel, the degradation and reassembly chemistry of iron−sulfur clusters via DNICs has been successfully mimicked in model studies.[4]

To understand the functions of DNICs, elucidation of their electronic structures is a prerequisite. Due to the well-known noninnocent nature of NO ligands, there is a longstanding debate about the electronic structures of DNICs. Several alternative electronic structures ($Fe^{I}(^{2}NO^{\bullet})_2$,[2b,4a,5] $Fe^{-I}(^{1}NO^{+})_2$,[6] or resonance hybrids of $Fe^{I}(^{2}NO^{\bullet})_2$ and $Fe^{III}(^{3}NO^{-})_2$[7]) have been proposed for $\{Fe(NO)_2\}^9$ (in the notation introduced by Enemark and Feltham[8]) $S_t = {}^1/_2$ core. Thus, the electronic structure of $\{Fe(NO)_2\}^9$ has not been unambiguously determined. The same holds true for the one-electron reduced form $\{Fe(NO)_2\}^{10}$.

Recently a series of DNICs ($\{Fe(NO)_2\}^9$ (**1**) and $\{Fe(NO)_2\}^{10}$ (**2**)) have been isolated and structurally as well as spectroscopically characterized.[4d] However, the experimental results appear to provide conflicting electronic structure information. The observed isomer shifts (Table 1) fall into a region of the isomer shift/oxidation state correlation diagram where different redox states heavily overlap,[9] thus preventing an unambiguous oxidation state assignment. Given the essentially identical isomer shifts for both species, the measurements would appear to imply a *ligand*-centered reduction. This would be consistent with *elongated* N−O bonds in **2** and considerable red shifts of the NO stretching frequencies (ν(NO)) upon reduction (Table 1), because in an NO-based reduction, the extra electron would occupy an NO-π* orbital. Thus, one would anticipate elongated Fe−N (NO) bonds in **2** due to the attenuated backbonding of the reduced NO ligands. However, the crystal structure of **2** exhibits *shorter* rather than the expected longer Fe−N (NO) bonds compared to **1**.

To address the intriguing question of whether the reduction is a metal- or ligand-centered process, the electronic structures of **1** and **2** have been investigated by DFT methods. Calculations were performed with the BP86,[10] TPSS,[11] B3LYP,[12] and TPSSh[13] density functionals. Quite surprisingly, only the TPSSh calculated Mössbauer parameters match experiment (Table 1 and S2). Thus, the TPSSh Kahn−Sham solutions were used to interpret the electronic structures of **1** and **2**.

For both species the computed geometries and Mössbauer spectroscopic parameters (isomer shifts, (δ) and quadrupole splittings (ΔE_Q)) are in excellent agreement with experiment. The calculations predict substantial red shifts of the NO stretching frequencies in **2** compared to **1**. The slight overestimation of the calculated frequency is not considered to be critical[5] since calculated harmonic frequencies are compared to experimental fundamentals.

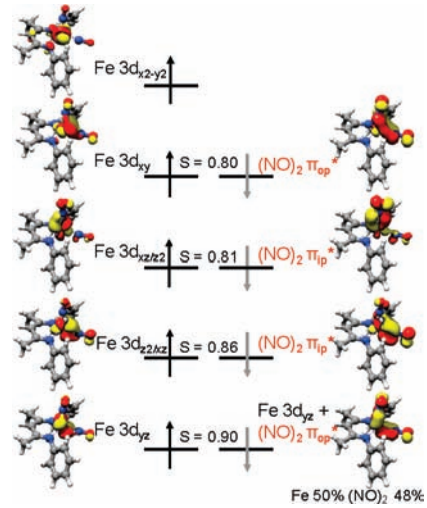

Figure 1. Schematic MO diagram for **1**.

Table 1. Comparison of the Calculated Structural and Spectroscopic Parameters for **1** and **2** with the Experimental Findings

	Fe−N (nacnac) Å	Fe−N (NO) Å	N−O Å	δ (mm/s)	$\lvert\Delta E_Q\rvert$ (mm/s)	ν(NO) (cm^{-1})
1 Calc.	1.998	1.705	1.174	0.22	0.83	1775
	1.996	1.714	1.171			1822
1 Exp.[4d]	1.974	1.696	1.177	0.19	0.79	1709
	1.968	1.688	1.174			1761
2 Calc.	2.055	1.679	1.204	0.25	1.21	1639
	2.052	1.679	1.199			1684
2 Exp.[4d]	2.053	1.668	1.218	0.22	1.31	1567
	2.051	1.649	1.191			1627

Due to the effective C_s symmetry of the complexes, the in-plane (ip) π*-orbitals (a′) of the two NO ligands cannot mix with their out-of-plane (op) counterparts (a″). Thus, symmetry dictates the formation of in-phase and out-of-phase combinations of the two NO-π_{ip}* orbitals, and the same holds true for the two NO-π_{op}* orbitals. Each combination of the NO π*-orbitals may interact with an Fe-3d fragment orbital of appropriate symmetry. A molecular orbital (MO) diagram for **1** is depicted in Figure 1. In the upper valence region one can readily identify five singly occupied spin-up MOs that are mainly of Fe-3d character. Four of them are bonding MOs that are shared between the iron center and the two NO ligands, while the last one is weakly π-antibonding with the supporting ligand (nacnac). In the spin-down manifold four unpaired electrons reside in the four NO π*-based orbitals thus yielding four spin-coupled pairs with the four spin-up iron-based MOs. In fact, one spin-down MO contains nearly identical contributions from the metal and the NO ligands (50% Fe vs 48% $(NO)_2$). Therefore, the bonding pattern is best rationalized by two resonance structures: (a) a high-spin (HS) ferric center ($S_{Fe} = {}^5/_2$) antiferromagnetically

 10.1021/ja9091616

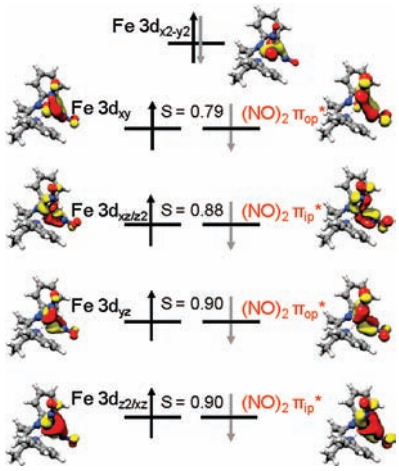

Figure 2. Schematic MO diagram for **2**.

coupled to two triplet NO^- ($S_{NO} = 1$) and (b) a HS ferrous ion ($S_{Fe} = 2$) bound to an overall $(NO)_2^-$ ligand with $S_{(NO)_2} = {}^3/_2$ in an antiferromagnetic fashion. This electronic structure description is consistent with the X-ray absorption experiments on similar $\{Fe(NO)_2\}^9$ species.[7b] The very large mutual spatial overlaps ($S = 0.8-0.9$) in all spin-coupled pairs demonstrates the highly covalent nature of the Fe−NO bonds.

The MO diagram for **2** (Figure 2) features a similar bonding situation to the one described for **1**. However, in **2** the weakly π-antibonding Fe-$d_{x^2-y^2}$ orbital is doubly occupied. The MOs in the spin-up manifold are mainly Fe-3d based orbitals, while the spin-down MOs are all of predominantly NO π*-character in contrast with the observations made for **1**. Hence, the electronic structure of **2** may best be described as consisting of a HS ferrous ion ($S_{Fe} = 2$) antiferromagnetically coupled to two triplet NO^- ligands ($S_{NO} = 1$) thus yielding an overall singlet ground state. Given the ambiguous oxidation state of the iron center in **1**, one may simply argue that it is not possible to determine whether the reduction is a metal- or ligand-centered process. However, in line with an earlier suggestion,[14] the process is still best viewed as a metal-based reduction, because the Fe-$d_{x^2-y^2}$ orbital acts as the electron acceptor. This is consistent with the elongated Fe−N (nacnac) bonds in **2** relative to **1** since the Fe-$d_{x^2-y^2}$ MO is a weakly π-antibonding orbital with respect to the Fe−N (nacnac) interaction.

The metal 3d-orbitals in **2** are energetically closer to the NO π*-orbitals than those in **1** because of the lower effective nuclear charge of the reduced metal center; therefore, the $\{Fe(NO)_2\}^{10}$ species features more pronounced π-backbonding. This results in the observed shorter Fe−N (NO) and longer N−O bonds in **2**, concomitant with the appreciable red shifts of the NO stretching frequencies. In other words, the reduced metal ion is a better electron donor into the NO π*-orbitals. As found in **2**, the reduction eventually yields a ferrous center bound to two NO^- ligands ($Fe^{II}-(NO^-)_2$).

Iron-based reductions usually lead to a substantial *increase* in isomer shifts (IS) because they are typically associated with considerable metal−ligand bond lengthening. However, similar ISs for **1** and **2** were observed. In addition to the oxidation state of the metal, ISs correlate strongly with the backbonding abilities of ligands: the stronger the π-backbonding, the smaller the IS.[15] Therefore, the two counteracting factors (the increasing number of d-electrons and the enhanced π-backbonding) lead to the only marginally increased IS for **2**.

In conclusion, experimentally calibrated electronic structure descriptions of the $\{Fe(NO)_2\}^9$ core and its one-electron reduced form, $\{Fe(NO)_2\}^{10}$, were reached by a detailed analysis of Kohn−Sham solutions that successfully reproduce the experimental structures and spectroscopic parameters. The $\{Fe(NO)_2\}^9$ unit is best described by two resonance structures consisting of a HS-Fe^{III} ($S_{Fe} = {}^5/_2$) bound to two triplet NO^- ligands ($S_{(NO)_2} = 2$) in an antiferromagnetic fashion and a HS-Fe^{II} ($S_{Fe} = 2$) antiferromagnetically coupled to an overall quartet $^4(NO)_2^-$ ligand ($S_{(NO)_2} = {}^3/_2$). The $\{Fe(NO)_2\}^{10}$ species contains a HS ferrous center ($S_{Fe} = 2$) antiferromagnetically coupled to two triplet NO^- ligands ($S_{(NO)_2} = 2$). The electronic structure of DNICs features highly covalent bonding between the iron center and the two NO ligands. As a consequence, four of the five Fe-3d orbitals are strongly π-bonding with respect to the Fe−NO interaction, while the last Fe 3d-based orbital remains essentially nonbonding. The latter acts as the electron acceptor orbital for the one-electron reduction of the $\{Fe(NO)_2\}^9$ species. This unusual "one-above-four" ligand field splitting pattern may have mechanistic implications for the reactivity of DNICs including modification and repair chemistry of iron−sulfur clusters.

Acknowledgment. The authors gratefully acknowledge a grant from the German Science Foundation (NE 690/7-1) and financial support from the special research unit SFB 813. We are indebted to Dr. Gemma Christian for helpful comments on the manuscript.

Supporting Information Available: Computational details, the results from all investigated density functionals, the MO diagrams for **1** and **2** from the BP86 and B3LYP calculations. This material is available free of charge via the Internet at http://pubs.acs.org.

References

(1) (a) Murad, F. *Angew. Chem., Int. Ed.* **1999**, *38*, 1856–1868. (b) Furchgott, R. F. *Angew. Chem., Int. Ed.* **1999**, *38*, 1870–1880. (c) Ignarro, L. J. *Angew. Chem., Int. Ed.* **1999**, *38*, 1882–1892.
(2) (a) Sellers, V. M.; Johnson, M. K.; Dailey, H. A. *Biochemistry* **1996**, *35*, 2699–2704. (b) Foster, M. W.; Cowan, J. A. *J. Am. Chem. Soc.* **1999**, *121*, 4093–4100.
(3) (a) Ding, H.; Demple, B. *Proc. Natl. Acad. Sci. U.S.A.* **2000**, *97*, 5146–5150. (b) Rogers, P. A.; Ding, H. *J. Biol. Chem.* **2001**, *276*, 30980–30986. (c) Yang, W.; Rogers, P. A.; Ding, H. *J. Biol. Chem.* **2002**, *277*, 12868–12873.
(4) (a) Tsai, M.-L.; Chen, C.-C.; Hsu, I.-J.; Ke, S.-C.; Hsieh, C.-H.; Chiang, K.-A.; Lee, G.-H.; Wang, Y.; Chen, J.-M.; Lee, J.-F.; Liaw, W.-F. *Inorg. Chem.* **2004**, *43*, 5159–5167. (b) Harrop, T. C.; Tonzetich, Z. J.; Reisner, E.; Lippard, S. J. *J. Am. Chem. Soc.* **2008**, *130*, 15602–15610. (c) Lu, T.-T.; Huang, H.-W.; Liaw, W.-F. *Inorg. Chem.* **2009**, *48*, 9027–9035. (d) Tonzetich, Z. J.; Do, L. H.; Lippard, S. J. *J. Am. Chem. Soc.* **2009**, *131*, 7964–7965.
(5) Dai, R. J.; Ke, S. C. *J. Phys. Chem. B* **2007**, *111*, 2335–2346.
(6) (a) Bryar, T. R.; Eaton, D. R. *Can. J. Chem.* **1992**, *70*, 1917–1926. (b) Butler, A. R.; Megson, I. L. *Chem. Rev.* **2002**, *102*, 1155–1165.
(7) (a) Hopmann, K. H.; Ghosh, A.; Noodleman, L. *Inorg. Chem.* **2009**, *48*, 9155–9165. (b) Tsai, M.-C.; Tsai, F.-T.; Lu, T.-T.; Tsai, M.-L.; Wei, Y.-C.; Hsu, I.-J.; Lee, J.-F.; Liaw, W.-F. *Inorg. Chem.* **2009**, *48*, 9579–9591.
(8) Enemark, J. H.; Feltham, R. D. *Coord. Chem. Rev.* **1974**, *13*, 339–406.
(9) Gütlich, P.; Link, R.; Trautwein, A. X. *Mössbauer Spectroscopy and Transtion Metal Chemistry*; Springer-Verlag: Berlin, 1978.
(10) (a) Becke, A. D. *Phys. Rev. A* **1988**, *38*, 3098–3100. (b) Perdew, J. P. *Phys. Rev. B* **1986**, *34*, 7406.
(11) (a) Tao, J.; Perdew, J. P.; Staroverov, V. N.; Scuseria, G. E. *Phys. Rev. Lett.* **2003**, *91*, 146401. (b) Perdew, J. P.; Tao, J.; Staroverov, V. N.; Scuseria, G. E. *J. Chem. Phys.* **2004**, *120*, 6898–6911.
(12) (a) Becke, A. D. *J. Chem. Phys.* **1993**, *98*, 5648–5652. (b) Lee, C. T.; Yang, W. T.; Parr, R. G. *Phys. Rev. B* **1988**, *37*, 785–789.
(13) Staroverov, V. N.; Scuseria, G. E.; Tao., J.; Perdew, J. P. *J. Chem. Phys.* **2003**, *119*, 12129–12137.
(14) Atkinson, F. L.; Blackwell, H. E.; Brown, N. C.; Connelly, N. G.; Crossley, J. G.; Orpen, A. G.; Rieger, A. L.; Rieger, P. H. *J. Chem. Soc., Dalton Trans.* **1996**, 3491–3502.
(15) Li, M.; Bonnet, D.; Bill, E.; Neese, F.; Weyhermüller, T.; Blum, N.; Sellmann, D.; Wieghardt, K. *Inorg. Chem.* **2002**, *41*, 3444–3456.

JA9091616